

Modeling unsteady friction in rapid transient pipe flows

H. A. Warda, H. A. Kandil, A. A. Elmilgui and E. M. Wahba
Mechanical Eng. Dept., Faculty of Eng., Alexandria University, Alexandria, Egypt

Accurate monitoring of pressure transients in pipes through a well-developed numerical model is a necessity for design engineers. The simple Method Of Characteristics (MOC) has been the standard method for modeling transients for the last five decades. However, complex phenomena such as unsteady friction cause strong distortion of the pressure waves travelling through fluid lines to that predicted by the standard MOC. Unfortunately, there is no universal unsteady friction model that can be used for both laminar and turbulent flows. This study is concerned with finding a universal model for unsteady friction that can be implemented in the MOC for both laminar and turbulent flows. The desired model must use a reasonable computer time and memory. In this study, unsteady friction is simulated using three different models available in the literature. The results are compared with experimental measurements and some modifications are introduced in order to reach a universal model capable of accurately and efficiently simulating unsteady friction. An experimental setup was constructed to obtain reliable experimental data to verify the modified numerical model for viscoelastic pipes. Also, experimental data from the available literature were used to verify the model for transient flows in elastic pipes. The results showed that unsteady friction is the main reason for damping the pressure transients in elastic pipes while it has a minor effect in viscoelastic pipes. Finally, the numerical model was verified experimentally to be capable of dealing with the pressure transients in the presence of unsteady friction in elastic pipes.

من الضروري استخدام نموذج رياضي دقيق لحساب ومتابعة الضغوط العابرة في المواسير أثناء عملية تصميم خطوط الأنابيب وشبكات المواسير. وخلال الخمسين عاما الماضية كانت طريقة الخصائص البسيطة تعتبر الطريقة القياسية التي تستخدم لمحاكاة الضغوط العابرة. ولكن هناك بعض الظواهر المعقدة مثل الاحتكاك غير المستقر والتي لا يمكن لطريقة الخصائص البسيطة محاكاتها مما يسبب اختلافا كبيرا بين القياسات العملية والنتائج التي يتم الحصول عليها باستخدام هذه الطريقة خاصة بعد مرور الموجة التضاغطية الأولى مما جعل الحاجة ملحة لتطوير النموذج الرياضي لزيادة دقته. وللأسف فإنه لا يوجد نموذج رياضي موحد للاحتكاك غير المستقر يمكن استخدامه في جميع أطوار السريان من سريان طبقي إلى سريان اضطرابي حيث أن كل نموذج يناسب أحد أطوار السريان فقط. في هذا البحث تمت محاولة لإيجاد نموذج موحد يمكن إدماجه في طريقة الخصائص التقليدية حتى يمكنها محاكاة الاحتكاك غير المستقر في جميع أطوار السريان وهذا النموذج يجب أن يستخدم أقل سعة تخزين وأقل زمن تشغيل عند استخدامه على الحاسب الآلي. في هذا البحث تمت محاكاة الاحتكاك غير المستقر في المواسير باستخدام ثلاثة نماذج مختلفة من النماذج المنشورة في المراجع والأبحاث السابقة. تم اختبار كل نموذج على مدى كبير من أرقام رينولدز التي تغطي أطوار السريان المختلفة وتمت مقارنة النتائج مع القياسات العملية حيث تم تحديد النموذج الذي يعطي أفضل النتائج ثم تم تعديل هذا النموذج حتى يمكن استخدامه بكفاءة ودقة في جميع أطوار السريان. للتحقق من صحة ودقة النموذج الذي تم تطويره في هذا البحث فقد تم إنشاء جهاز معلمي قادر على توفير نتائج معملية دقيقة للسريان العابر في المواسير ذات المرونة اللزجة كذلك تم استخدام النتائج المعملية المتوفرة في المراجع الأخرى للتحقق من صحة النموذج الرقمي في حالة المواسير المرنة. نتائج التحليل أوضحت أن الاحتكاك غير المستقر هو السبب الرئيسي لتضاؤل الموجات التضاغطية في المواسير المرنة ولكن تأثيره مهمل على تضاؤل الموجات التضاغطية في المواسير ذات المرونة اللزجة. وبالتالي تم التحقق من قدرة النموذج المعدل لطريقة الخصائص على محاكاة السريان العابر في المواسير أخذاً في الاعتبار تأثير جميع الظواهر السابق ذكرها.

Keywords: Unsteady flow in pipes, Water hammer, Unsteady friction, Pressure transients

1. Introduction

The Method Of Characteristics (MOC) was first proposed by Rieman in 1860. Studies covering the application of the MOC to unsteady flow and water hammer problems

developed continuously over the last 50 years. For example, Watters [1] provided the detailed theoretical basis for estimating the wave speed in different types of conduits. Also, Wylie and Streeter [2] summarized the various methods of solution for the water hammer problem.

They stated that the MOC is considered to be the standard numerical method by which other methods may be judged for accuracy and efficiency in modeling pressure transients. Kaplan et al. [3] showed that transients arising in long oil pipelines could be adequately simulated by the MOC. On the other hand, Bergant and Simpson [4] demonstrated the numerical inaccuracies that could arise from applying the standard MOC for boundaries such as valves, orifices and centrifugal pumps. A basis for verifying the accuracy of numerical techniques applied to transient flow in pipe systems was presented by Boulos, Wood and Funk [5].

In all the studies mentioned above, a noticeable distortion was observed between the experimental data and the results of the numerical models based on the MOC. One of the major causes of the deviation is the poor modeling of unsteady friction through the quasi-steady approximation that evaluates the instantaneous shear stress by the value that would apply at the same mean velocity in a steady flow. This fact attracted many researchers to improve the modeling of unsteady friction.

For example, Zielke [6] developed a weighting-function model, for friction losses in transient laminar pipe flow, based on an exact analytical solution of laminar flow equations. He found that frequency-dependant friction is only one of several causes of distortion effects and that the viscoelastic behavior of the pipe may be of importance. However, Zielke's technique has a major drawback because it requires a very large amount of computational time and computer storage capacity. Later, the computational time and computer storage required to implement Zielke's model was greatly reduced by Trikha [7]. Also, Suzuki et al. [8] presented an alternative approach for improving Zielke's weighting function model in laminar flow of liquids in pipes.

Vardy and Hwang [9] developed a quasi two-dimensional model for transient flows in pipes using the one-dimensional MOC in concentric cylindrical annuli. They applied the model to laminar flows and to a five-region model of turbulent flow. Later, Vardy et al. [10] developed a weighting function model for transient turbulent pipe friction at moderate Reynolds numbers in a manner similar to

Zielke's expression for laminar flows. Another weighting-function model for transient turbulent friction in smooth pipes was developed by Vardy and Brown [11]. They claimed that the model gives results equivalent to Zielke's model in laminar flows.

Another model was developed by Brunone et al. [12] who suggested that both local inertia and friction forces depend on the same quantities in fast transients. Therefore, they proposed a single expression for both effects. This expression is in the form of an additional term to the friction term in the momentum equation. To apply this expression, Brunone et al. [13] introduced a modified characteristic method where they applied the usual equations of the MOC and evaluated the new added term in an explicit manner. Brunone et al. [14] applied a two-dimensional model to expand the limited experimental data available with numerical results, and they obtained useful information on the evolution of the velocity profiles during a transient.

An alternative approach for the computation of unsteady friction losses for both laminar and turbulent flows was developed by Silva-Araya and Chaudhry [15]. The approach is based on the energy dissipation factor, which is defined as the ratio of energy dissipation in transient flow to the energy dissipation in quasi-steady conditions. However, computational time and memory requirements of the energy dissipation model are about three orders of magnitude larger than those of the quasi-steady approximation.

From the previous review, it is noted that there is no universal model that is capable of handling the complex water hammer problem in the presence of unsteady friction for both laminar and turbulent flows in the MOC. Therefore, this study has to look for a suitable model for unsteady friction that can be implemented in the MOC. The desired model must use a reasonable computer time and memory. To achieve this goal, three of the unsteady friction models mentioned above are applied to laminar and turbulent flow cases. The results are compared with experimental measurements and some modifications are introduced in order to reach a universal model capable of accurately and efficiently simulating unsteady friction for both laminar and turbulent flows. The MOC will then be

modified to employ the universal unsteady friction model.

2.1. Standard method of characteristics

The governing equations are given in Watters [1] as follows:

Continuity equation,

$$\frac{1}{\rho} \frac{dP}{dt} + a^2 \frac{\partial V}{\partial s} = 0 \quad (1)$$

Euler (Momentum) equation,

$$\frac{dV}{dt} + \frac{1}{\rho} \frac{\partial P}{\partial s} + g \frac{dz}{ds} + \frac{f}{2D} V|V| = 0 \quad (2)$$

Introducing (λ) as a linear scale factor, the governing equations may be combined in one equation. as follows:

$$\lambda \left(\frac{dV}{dt} + \frac{1}{\rho} \frac{\partial P}{\partial s} + g \frac{dz}{ds} + \frac{f}{2D} V|V| \right) + a^2 \frac{\partial V}{\partial s} + \frac{1}{\rho} \frac{dP}{dt} = 0 \quad (3)$$

By breaking the terms (dV/dt) and (dP/dt) down into their components and regrouping terms, the equation becomes:

$$\left(\lambda \frac{\partial V}{\partial t} + (\lambda V + a^2) \frac{\partial V}{\partial s} \right) + \left(\frac{1}{\rho} \frac{\partial P}{\partial t} + \left(\frac{V}{\rho} + \frac{\lambda}{\rho} \right) \frac{\partial P}{\partial s} \right) + \lambda g \frac{dz}{ds} + \frac{\lambda f}{2D} V|V| = 0 \quad (4)$$

Some manipulations are then performed to this equation to replace the original two partial differential equations with two ordinary differential equations as follows:

$$\frac{dV}{dt} + \frac{g}{a} \frac{dH}{dt} - \frac{g}{a} V \frac{dz}{ds} + \frac{f}{2D} V|V| = 0,$$

for $\frac{ds}{dt} = V + a \quad (5)$

and

$$\frac{dV}{dt} - \frac{g}{a} \frac{dH}{dt} + \frac{g}{a} V \frac{dz}{ds} + \frac{f}{2D} V|V| = 0,$$

for $\frac{ds}{dt} = V - a \quad (6)$

Where the pressure (P) was replaced by $\rho g(H-z)$.

Eq. (5) is usually known as the C^+ characteristic equation while eq. (6) is known as the C^- characteristic equation. Eqs. (5 and 6) can now be expressed in a finite difference form based on fig. 1, as follows:

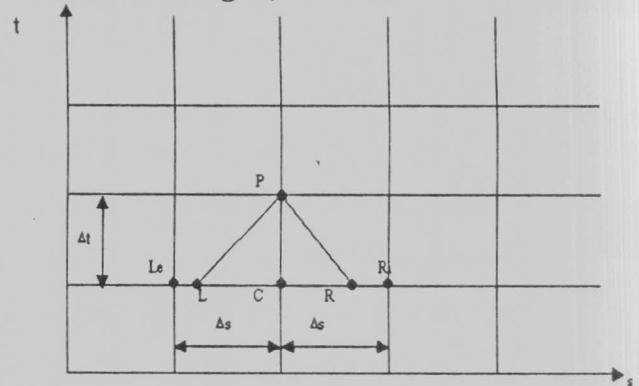


Fig.1. Rectangular grid in the (s-t) plane.

The C^+ equation becomes,

$$\frac{V_P - V_L}{\Delta t} + \frac{g}{a} \frac{H_P - H_L}{\Delta t} - \frac{g}{a} V_L \frac{dz}{ds} + \frac{fV_L|V_L|}{2D} = 0 \quad (7)$$

The C^- equation becomes,

$$\frac{V_P - V_R}{\Delta t} - \frac{g}{a} \frac{H_P - H_R}{\Delta t} + \frac{g}{a} V_R \frac{dz}{ds} + \frac{fV_R|V_R|}{2D} = 0 \quad (8)$$

In applying the finite difference numerical analysis, the pipe has to be divided into a number of sections. Grid points along the s -axis represent points spaced (Δs) apart along the pipe.

In order to determine the values of (H) and (V) at various selected nodes along the pipe, initial conditions along the s -axis (at $t = 0$) and boundary conditions for all times at the pipe ends, $s = 0$ and $s = L$, should be known. The initial conditions are generally some steady state flow situation in the pipe. The boundary conditions at each end of the pipe are comprised of externally imposed conditions of velocity and/or pressure head. In this study, the boundaries of the pipe are an upstream

reservoir boundary condition and a downstream boundary of a rapidly closing solenoid valve.

At the upstream reservoir, the value of H is assumed to remain constant throughout the time of simulation that is expressed as; $H_{P1} = H_0$. The velocity at the upstream boundary could be obtained from the C-characteristic equation as follows,

$$V_{P1} = V_R + \frac{g}{a}(H_0 - H_R) - \frac{g\Delta t}{a} V_R \frac{dz}{ds} - \frac{f\Delta t}{2D} V_R |V_R|. \quad (9)$$

The downstream boundary is a rapidly closing solenoid valve that will generate the pressure transient within the system. This boundary is modeled using the method proposed by Wahba [16].

2.2. Verification of the MOC

In order to test the capability of the MOC in modeling the unsteady flow in a pipe, an experimental setup was constructed in the Fluid Mechanics Laboratory at the Faculty of Engineering, Alexandria University. The setup, shown schematically in fig. 2, consists of a PVC pipe of 25.4 mm. inside diameter, 4.2 mm. thickness and 25.6 m. length. The upstream end of the pipe is connected to a constant-head, 9-cubic-meter-capacity tank which holds a maximum head of 11 meters above the pipe centerline. A normally-closed solenoid-operated valve, with a closure time of 0.08 seconds, is fitted at the downstream end of the pipe.

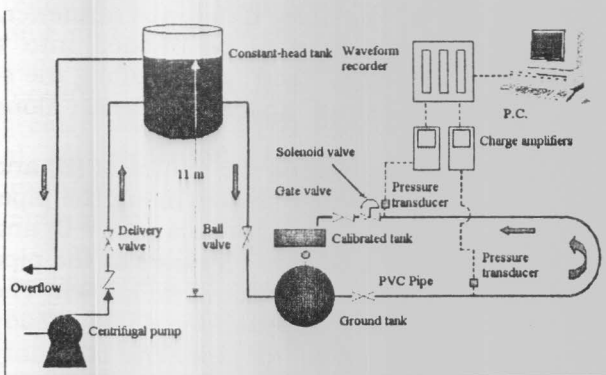


Fig. 2. Diagrammatic sketch of the experimental setup.

To verify the MOC for laminar flow, a flow case corresponding to a Reynolds Number of 1575, was carried out in the laboratory and then simulated by the numerical model. The results predicted by the standard MOC model are compared with the experimental data. The results of the comparison are shown in fig. 3. The comparison in fig. 3 shows that the standard MOC model is not capable of reproducing the pressure oscillations following the first pressure peak. This is due to the inefficient simulation of the damping mechanism through the standard MOC model. For more investigation, a turbulent flow case, at a Reynolds number of 7240, was also simulated using the MOC model. A comparison between the results of the standard MOC model and the experimental data for this case is shown in fig. 4.

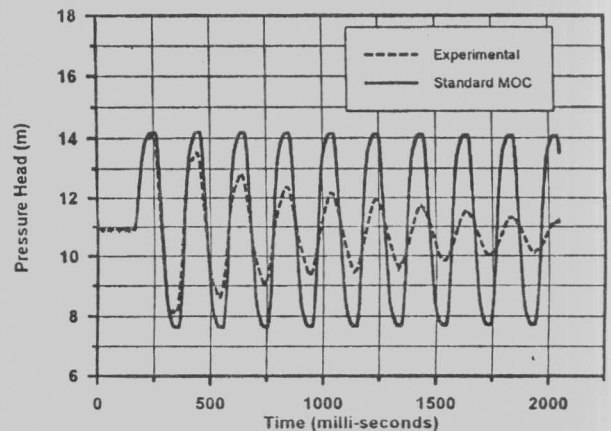


Fig. 3. Verification of the standard MOC for laminar flow, $R_N = 1575$.

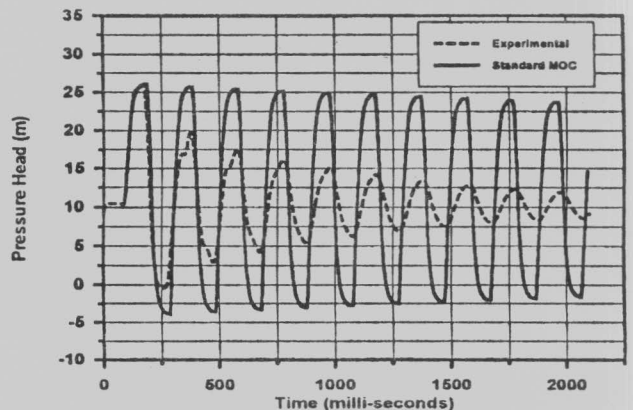


Fig. 4. Verification of the standard MOC for turbulent flow, $R_N = 7240$.

The comparison in fig. 4 again confirms that the standard MOC model is only capable of modeling the first pressure peak and to an extent the frequency of the propagated wave. However, the damping of the subsequent peaks is grossly underestimated. In other words, the standard MOC model only allows modeling of the maximum pressure values, which usually occur at or before the end of the valve closure maneuver. On the contrary, the attenuation of the pressure peaks happening after the end of the valve closure is not accurately predicted by the model. This is because the unsteady friction term is estimated through steady state relationships. Therefore, an efficient model for transient friction should be embedded in the MOC model to overcome this drawback.

3.1. Unsteady friction models for laminar flow

In this section, the unsteady friction models used in this study are presented.

3.1.1. Zielke's model

Zielke [6] developed his model by solving the equation of motion for parallel axisymmetric flow of an incompressible fluid. This solution takes the following form:

$$h_f(t) = \frac{8\nu}{gR^2} V(t) + \frac{4\nu}{gR^2} \int_0^t \frac{\partial V}{\partial t}(u) W(t-u) du \quad (10)$$

Where, R is the pipe radius, $h_f(t)$ is the friction head loss per unit length at time (t) from the beginning of the simulation, ν is the kinematic viscosity of the fluid, $\tau = \frac{\nu}{R^2} t$ is a dimensionless time, u is the time used in convolution integral, and $W(t) = \bar{W}(\tau)$ is a weighting function.

The weighting function $\bar{W}(\tau)$ could be calculated from the following equations:

$$\bar{W}(\tau) = e^{-26.3744\tau} + e^{-70.8493\tau} + e^{-135.0198\tau} + e^{-218.9216\tau} + e^{-322.5544\tau}$$

for $\tau > 0.02$, (11)

and

$$\bar{W}(\tau) = 0.282095 \tau^{-0.5} - 1.25 + 1.057855 \tau^{0.5} + 0.9375 \tau + 0.396696 \tau^{1.5} - 0.351563 \tau^2$$

for $\tau < 0.02$. (12)

Eq. (10) could be integrated by a first order approximation to obtain the friction head loss. By performing the integration over time $t = K\Delta t$ (after K time steps), the following equation is obtained:

$$h_f(K\Delta t) = \frac{8\nu}{gR^2} V_{i,K\Delta t} + \frac{4\nu}{gR^2} \sum_{J=1}^K [V_{i,(K-J+1)\Delta t} - V_{i,(K-J)\Delta t}] W\left[\left(J - \frac{1}{2}\right)\Delta t\right] \quad (13)$$

The C^+ and C^- characteristic equations, eqs. (5 and 6), may be rewritten in a more general form, excluding the quasi-steady approximation, as follows:

$$C^+ : V_P - V_L + \frac{g}{a}(H_P - H_L) - \frac{g\Delta t}{a} V_L \frac{dz}{ds} + gh_{fL}\Delta t = 0, \quad (14)$$

$$C^- : V_P - V_R - \frac{g}{a}(H_P - H_R) + \frac{g\Delta t}{a} V_R \frac{dz}{ds} + gh_{fR}\Delta t = 0. \quad (15)$$

For the quasi-steady approximation, the friction-loss terms are given by:

$$h_{fL} = \frac{fV_L|V_L|}{2gD} \quad \text{and} \quad h_{fR} = \frac{fV_R|V_R|}{2gD}$$

For Zielke's model, the friction-loss terms are given by:

$$h_{fL}(K\Delta t) = \frac{8\nu}{gR^2} V_{L,K\Delta t} + \frac{4\nu}{gR^2} \sum_{J=1}^K [V_{L,(K-J+1)\Delta t} - V_{L,(K-J)\Delta t}] W\left[\left(J - \frac{1}{2}\right)\Delta t\right], \quad (16)$$

and

$$h_{fR}(K\Delta t) = \frac{8v}{gR^2} V_{R,K\Delta t} + \frac{4v}{gR^2} \sum_{J=1}^K [V_{R,(K-J+1)\Delta t} - V_{R,(K-J)\Delta t}] W\left[\left(J - \frac{1}{2}\right)\Delta t\right]. \quad (17)$$

Where the weighting function is calculated at an intermediate time equals $\left(J - \frac{1}{2}\right)\Delta t$.

Therefore, by combining eqs. (11- 16 and 17), the MOC model now contains all terms needed for simulating transient friction for laminar flows.

The main disadvantage of this approach is that its use can be inconvenient in numerical analysis because data is required from many previous time steps. This difficulty was largely avoided by Trikha's approximation.

3.1.2. Trikha's method

Trikha [7] approximated eq. (10) by a short series of exponential expressions consisting of three terms as follows:

$$h_f(K\Delta t) = \frac{8v}{gR^2} V_{i,K\Delta t} + \frac{4v}{gR^2} [y_1(K\Delta t) + y_2(K\Delta t) + y_3(K\Delta t)].$$

Where,

$$y_i(K\Delta t) = y_i[(K - 1)\Delta t] e^{-n_i\left(\frac{v}{R^2}\right)\Delta t} + m_i e^{-n_i\left(\frac{v}{R^2}\right)\frac{\Delta t}{2}} [V_{i,K\Delta t} - V_{i,(K-1)\Delta t}],$$

and

$$y_i(t = 0) = 0.$$

The values of n_i and m_i are given in the following table:

i	n_i	m_i
1	26.4	1
2	200	8.1
3	8000	40

Therefore,

$$h_{fL}(K\Delta t) = \frac{8v}{gR^2} V_{L,K\Delta t} + \frac{4v}{gR^2} [y_{1L}(K\Delta t) + y_{2L}(K\Delta t) + y_{3L}(K\Delta t)]. \quad (18)$$

Where:

$$y_{iL}(K\Delta t) = y_{iL}[(K - 1)\Delta t] e^{-n_i\left(\frac{v}{R^2}\right)\Delta t} + m_i e^{-n_i\left(\frac{v}{R^2}\right)\frac{\Delta t}{2}} [V_{L,K\Delta t} - V_{L,(K-1)\Delta t}], \quad (19)$$

$$h_{fR}(K\Delta t) = \frac{8v}{gR^2} V_{R,K\Delta t} + \frac{4v}{gR^2} [y_{1R}(K\Delta t) + y_{2R}(K\Delta t) + y_{3R}(K\Delta t)]. \quad (20)$$

Where:

$$y_{iR}(K\Delta t) = y_{iR}[(K - 1)\Delta t] e^{-n_i\left(\frac{v}{R^2}\right)\Delta t} + m_i e^{-n_i\left(\frac{v}{R^2}\right)\frac{\Delta t}{2}} [V_{R,K\Delta t} - V_{R,(K-1)\Delta t}]. \quad (21)$$

By simultaneously solving eqs. (14, 15, 18, and 20), the required computational time as well as the computer storage capacity are dramatically reduced.

3.2. Unsteady friction models for turbulent flow

No exact solution exists for transient friction in turbulent pipe flows. The most promising models of unsteady friction in turbulent pipe flows are grouped into two categories. One uses the history of the flow, as applied by Vardy and Brown [11], while the other uses instantaneous conditions as presented by Brunone et al. [12] and Brunone et al. [14]. Verification of these two approaches with experimental data was not performed in any of the reviewed literature. Hence, Brunone et al.'s model together with the weighting function model presented by Vardy and Brown [11] are applied in this study for modeling unsteady friction in turbulent pipe flows.

3.2.1. Brunone et al. model

Brunone et al. [12] introduced an additional term in the momentum equation to model the effects of the flow field two-dimensionality in a one-dimensional formulation. This term was added to model the effects of both the local inertia and the unsteady friction on the flow. Hence, the momentum equation is modified to the following form:

$$\frac{dV}{dt} + \frac{1}{\rho} \frac{\partial P}{\partial s} + g \frac{dz}{ds} + \frac{f}{2D} V|V| + k \left(\frac{\partial V}{\partial t} - a \frac{\partial V}{\partial s} \right) = 0. \quad (22)$$

Where (k) is a suitable coefficient that has to be determined. They assumed that the modified momentum equation together with the continuity equation could be seen as the usual compatibility equations with a new term added that depends on partial derivatives of the mean velocity (V).

Therefore, the compatibility equations would take the following form,

$$C^+ : \frac{V_P - V_L}{\Delta t} + \frac{g}{a} \frac{H_P - H_L}{\Delta t} - \frac{g}{a} V_L \frac{dz}{ds} + \frac{fV_L|V_L|}{2D} + J_L = 0, \quad (23)$$

Where:

$$J_L = k \frac{V_L^{t-\Delta t} - V_L^{t-2\Delta t}}{\Delta t} - ak \frac{V_P^{t-\Delta t} - V_L^{t-\Delta t}}{\Delta s}, \quad (24)$$

and,

$$C^- : \frac{V_P - V_R}{\Delta t} - \frac{g}{a} \frac{H_P - H_R}{\Delta t} + \frac{g}{a} V_R \frac{dz}{ds} + \frac{fV_R|V_R|}{2D} + J_R = 0, \quad (25)$$

where:

$$J_R = k \frac{V_R^{t-\Delta t} - V_R^{t-2\Delta t}}{\Delta t} - ak \frac{V_R^{t-\Delta t} - V_P^{t-\Delta t}}{\Delta s}. \quad (26)$$

The major drawback of this model is the difficulty of determining a suitable value for the constant (k). However, Brunone et al. [14]

suggested that a first approximation for (k) could be assumed within the interval (0.03 - 0.1).

3.2.2. Vardy and brown model

Vardy and Brown [11] developed a weighting function (W) for unsteady friction in smooth pipe turbulent flow for the expression,

$$h_f(t) = \frac{fV^2}{4gR} + \frac{4v}{gR^2} \int_0^t \frac{\partial V}{\partial t} (u)W(t-u)du.$$

The weighting function takes the following form:

$$\bar{W}(\tau) = \left(\frac{1}{2\sqrt{\pi\tau}} \right) e^{-\tau/C^*}. \quad (27)$$

Where,

$$C^* = \text{Shear decay coefficient} = \frac{7.41}{R_N^b}, \quad (28)$$

and

$$b = \log_{10} \left(\frac{14.3}{R_N^{0.05}} \right). \quad (29)$$

For laminar flows, C* takes a constant value of 0.00476 irrespective of Reynolds number. The weighting function for turbulent flow is a function of Reynolds number.

By simultaneously solving eqs. (14-17) together with eqs. (27- 29), the MOC model is now capable of simulating transient friction in turbulent flows for smooth pipes. The advantage of this approach is that there is no need for empirical coefficients.

3.3. Verification of the unsteady friction models

The experimental measurements for the laminar flow case, $R_N = 1575$, are again compared with the results of the modified MOC model. The model is now modified for simulating transient friction in laminar flows through Trikha's approximation of Zielke's weighting function model. The results of the comparison are shown in fig. 5. Fig. 5 shows a

noticeable improvement in the simulation by the modified MOC model. However, the damping is still not accurately simulated. This implies that there is another damping mechanism of strong influence that is not taken into account through the present model. This damping mechanism is due to the viscoelastic behavior of the PVC pipe. In order to eliminate the effect of the viscoelasticity of the PVC pipe in which the measurements were taken, the modified model is used to reproduce the experimental data obtained for elastic pipes such as steel or copper pipes.

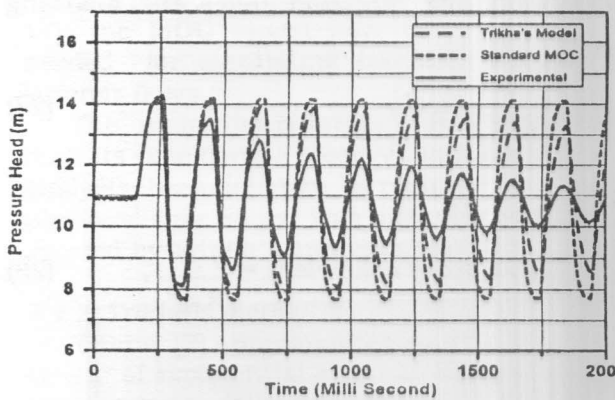


Fig. 5. Verification of the modified MOC for laminar flow.

Therefore, the second alternative is to use the available experimental data for unsteady flow in steel or copper pipes in the cited references. This was achieved through the experimental data provided by Holmboe and Rouleau [17].

Holmboe and Rouleau [17] performed their tests on a 0.025m-inner-diameter copper pipe. The upstream end of the pipe was connected to a constant head tank. A quick closing valve was mounted at the downstream end of the pipe. The pipe length is 36.09m, and it was embedded in concrete to reduce vibrations. Pressure transducers were mounted directly upstream of a quick closing valve and at the pipe midpoint.

Tests were performed with water and a high-viscosity oil ($\mu = 0.03484 \text{ N.s/m}^2$). The wave speed was 1350 m/s for water and it was 1324 m/s for the high viscosity oil. Reynolds number for oil was 82, representing a laminar flow case, and it was 6166 for water, representing a turbulent flow case.

3.4. Verification of the unsteady friction models for elastic pipes

3.4.1. Laminar flow

The modified MOC, using Trikha's unsteady friction model, is now used to simulate the pressure transient in the laminar flow of the high-viscosity oil. Numerical results from the modified MOC model are compared with the experimental results at the valve and at the midpoint, as shown in figs. 6- 7, respectively.

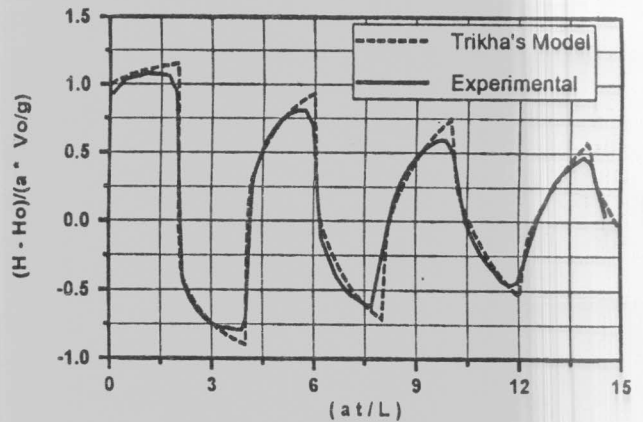


Fig. 6. Predicted pressure history by Trikha's model at the valve for laminar flow, $R_N = 82$.

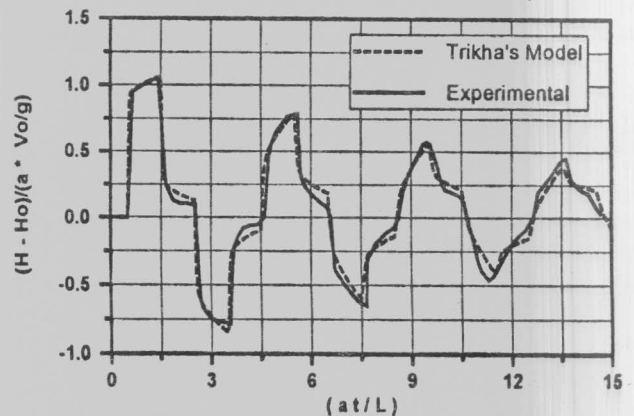


Fig. 7. Predicted pressure history by Trikha's model at the mid-point For laminar flow, $R_N = 82$.

Figs. 6 and 7 show good agreement between the experimental data and the modified MOC model, which was not the case for the viscoelastic PVC pipe.

3.4.2. Turbulent flow

The available experimental data for the turbulent flow case [17] was then simulated by the MOC model, utilizing Brunone et al. and Vardy et al.'s models for unsteady friction. A value of ($k = 0.02$) was applied for Brunone et al.'s model. The pressure oscillations obtained by the model of Brunone et al. are compared with the experimental data [17] and the results are shown in figs. 8 and 9.

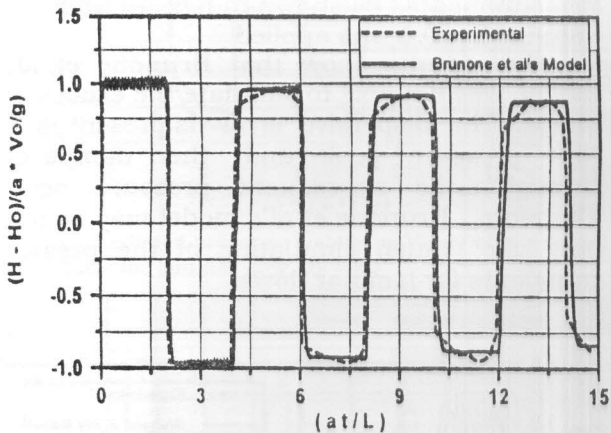


Fig. 8. Predicted pressure history by Brunone et al.'s model at the valve for the turbulent flow case, $R_N = 6166$.

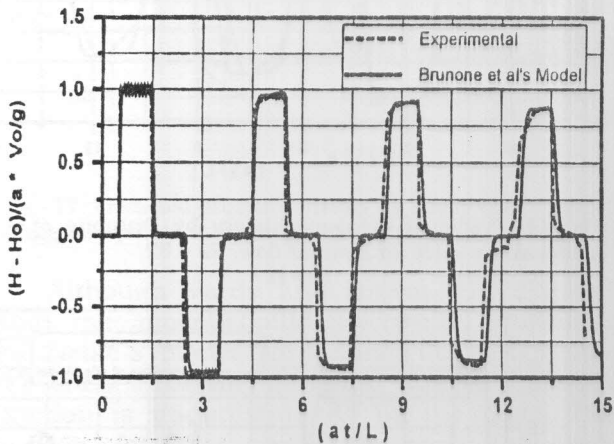


Fig. 9. Predicted pressure history by Brunone et al.'s model at the mid-point for turbulent flow.

Figs. 8 and 9 show that Brunone et al.'s model is capable of predicting the pressure transients. However, there is a dispersive error with the first pressure peak, both at the valve and at the midpoint. This dispersive error has damped out through the rest of the transient.

The model is also incapable of simulating the rounding of the pressure peaks.

Vardy et al.'s model [11] is also applied to simulate the pressure transients of the same turbulent-flow case. Results of the simulation are compared with the experimental measurements, as shown in figs. 10 and 11 for the pressure history at the valve and at the mid point, respectively.

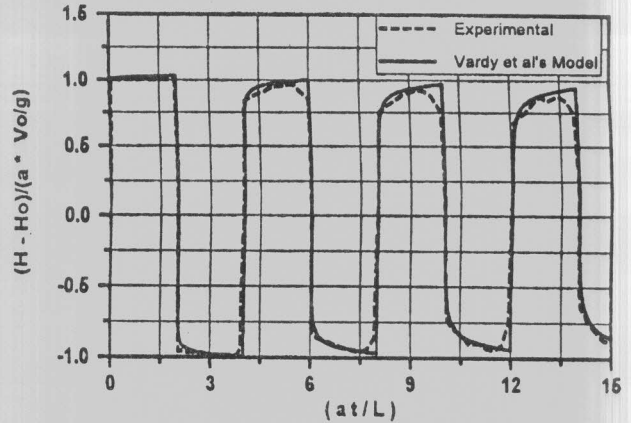


Fig. 10. Predicted pressure history by Vardy et al.'s model at the valve for turbulent flow, $R_N = 6166$.

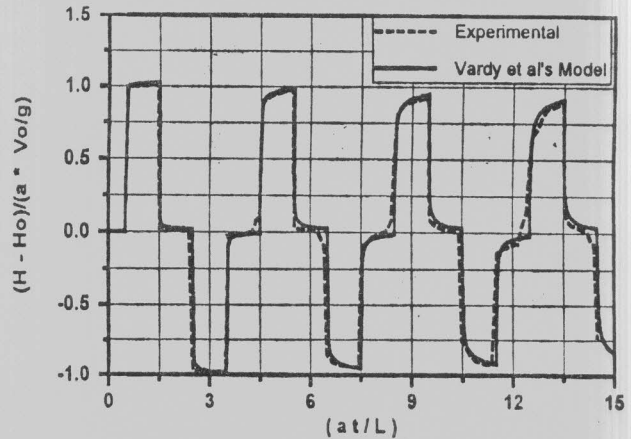


Fig. 11. Predicted pressure history by Vardy et al.'s model at the mid-point for turbulent flow, $R_N = 6166$.

Vardy et al.'s model shows a better agreement with the experimental data. No dispersive errors are present and there is no need for a calibrated constant. The rounding of the pressure peaks is clearly reproduced. However, the processing time for Vardy et al.'s model is much greater than that for Brunone et al.'s model. The difference in time increases as the number of nodes increases.

3.5. Finding the universal unsteady-friction model

The purpose of this section is to find the most suitable unsteady friction model that could be embedded into the standard MOC. To achieve this purpose, all the models under consideration will be tested for both laminar and turbulent flow cases. Trikha's method, originally developed for laminar flow, is tested against turbulent flow data while Brunone et al. and Vardy et al.'s models, originally developed for turbulent flow, are tested against laminar flow data.

Trikha's approximation of Zielke's weighting function model is applied to the turbulent flow case ($R_N = 6166$). Results of the comparison between the numerical and experimental pressure oscillations are shown in figs. 12- 13.

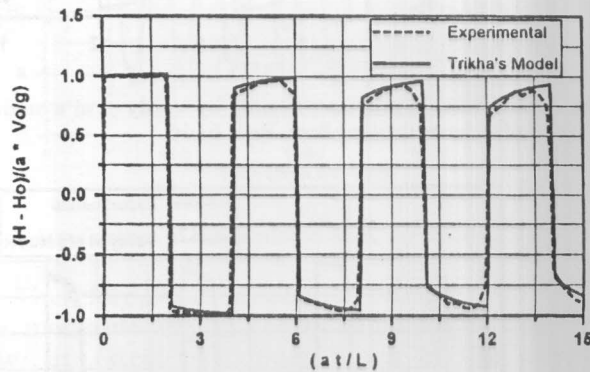


Fig. 12. Pressure history by Trikha's model at the valve for turbulent flow, $R_N = 6166$.

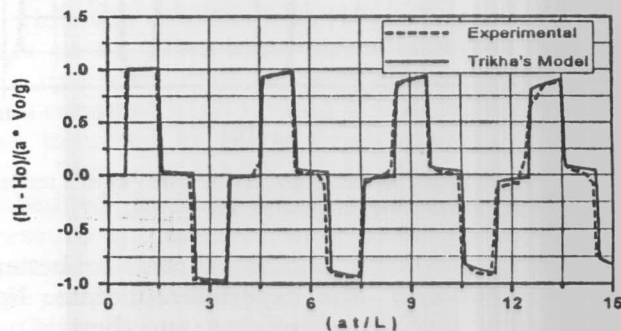


Fig. 13. Predicted pressure history by Trikha's model at the mid-point for turbulent flow, $R_N = 6166$.

Figs. 12 and 13 show that Trikha's approximation of Zielke's model is capable of

simulating unsteady friction for the turbulent flow case ($R_N = 6166$). This could justify the use of Trikha's method in modeling transient friction for laminar flows as well as low Reynolds number turbulent flows ($R_N 6200$) however, it is not recommended for high-Reynolds-number flows [7].

Brunone et al.'s model is then used to simulate Holmboe and Rouleau's [17] laminar flow case. Results of the simulation are compared with the experimental measurements, as shown in figs. 14 and 15. A value of $k = 0.1$ was applied.

The results show that Brunone et al.'s model was not able to simulate the exact wave shape. The dispersive error is present in the first pressure peak and then damps out through the subsequent pressure peaks. Therefore, Brunone et al.'s model may be used only for rough simulating of the pressure transients for laminar flows.

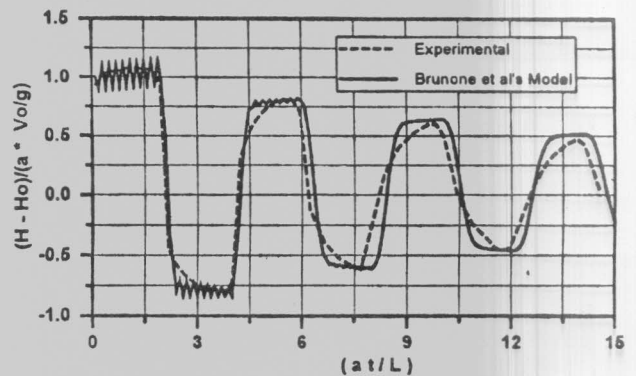


Fig. 14. Predicted pressure history by Brunone et al's model at the valve for laminar flow, $R_N = 82$.

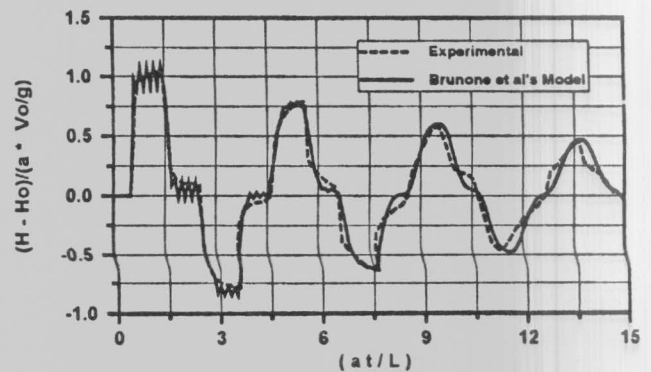


Fig. 15. Predicted pressure history by Brunone et al's model at the mid-point for laminar flow, $R_N = 82$.

Finally, Vardy et al.'s model is used to simulate Holmboe and Rouleau's laminar flow case. Results of the simulation are shown in figs. 16 and 17.

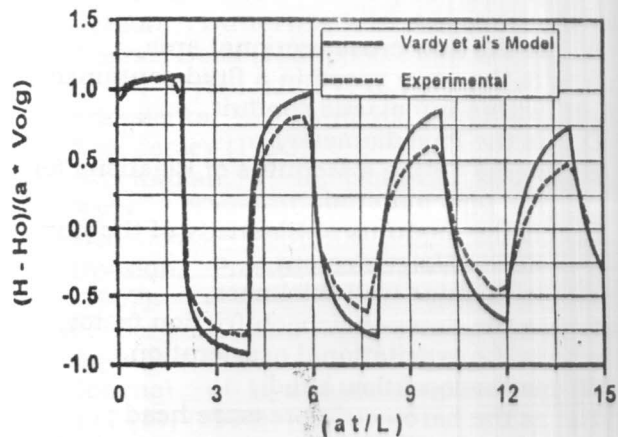


Fig. 16. Predicted pressure history by Vardy et al's model at the valve for laminar flow, $R_N = 82$.

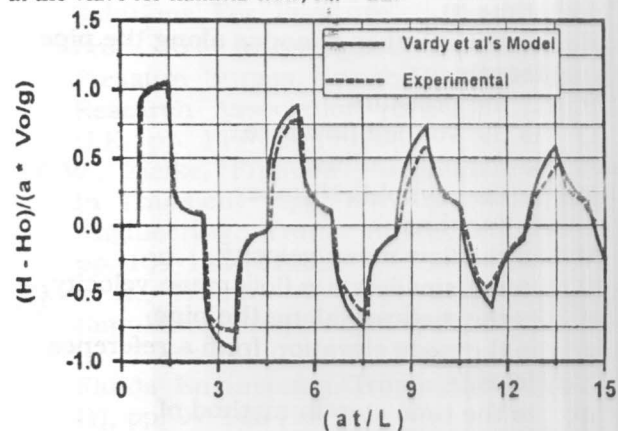


Fig. 17. Predicted pressure history by Vardy et al's model at the mid-point for the laminar flow case.

Although Vardy and Brown [11] claimed that the model should give results equivalent to Zielke's model for laminar flows, figs. 16 - 17 show that the damping due to transient friction is underestimated by the model. The reason for this could be seen if Zielke's weighting function is compared to Vardy et al.'s weighting function in case of a laminar flow ($C^* = 0.00476$).

The comparison between both weighting functions is shown in fig. 18. From fig. 18, it is clear that Vardy et al.'s weighting function for laminar flow has lower values in comparison with the analytically proved laminar flow

weighting function by Zielke, therefore, it underestimates the transient friction.

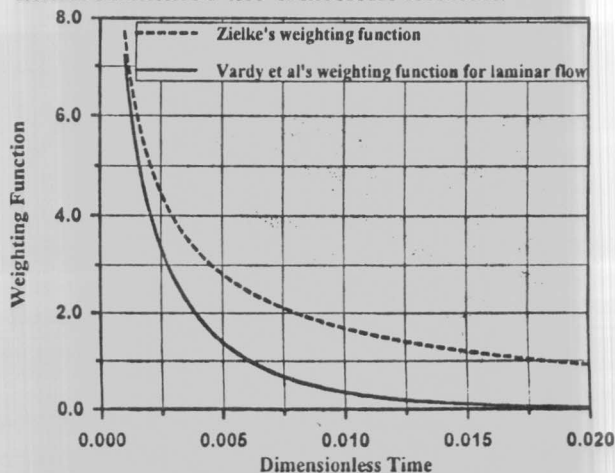


Fig. 18. Comparison between Vardy et al's weighting function and Zielke's weighting function for laminar flows.

This drawback could be overcome if a new value for the shear decay coefficient is determined for laminar flows. The new value for the shear decay coefficient could be estimated by fitting Vardy et al.'s weighting function for laminar flows to Zielke's weighting function. This curve fitting process was performed using a non-linear regression model and a new value for the shear decay coefficient, $C^* = 0.0215$, was obtained.

The results of reproducing Holmboe and Rouleau's laminar flow case [17], using this modified Vardy et al.'s model, are shown in figs. 19 and 20.

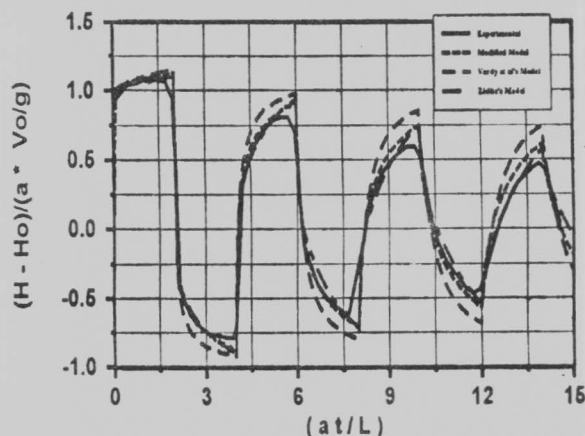


Fig. 19. Comparison between the different weighting function models for laminar flow at the valve.

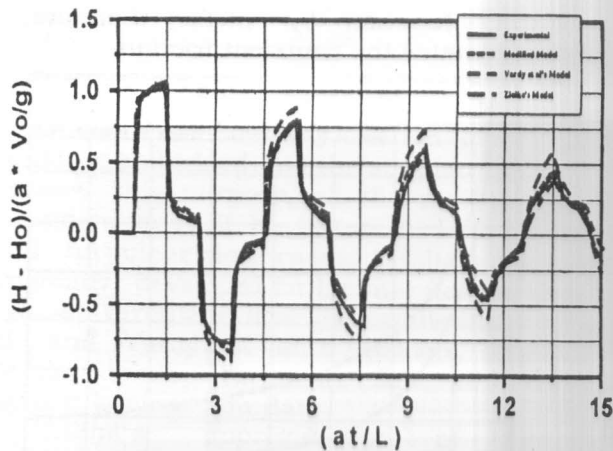


Fig. 20. Comparison between the different weighting function models for laminar flow at the mid-point.

The results in figs. 19 and 20 show that the modified unsteady friction model is capable of reproducing the experimental pressure oscillations for laminar flows.

4. Conclusions

Three unsteady friction models were applied for both laminar and turbulent flow cases and the following results were obtained:

- 1) Trikha's approximation of Zielke's weighting function, originally developed for laminar flow, can only be used for low-Reynolds-number turbulent flows but it is not recommended for high-Reynolds number flows.
- 2) Brunone et al.'s model, originally developed for turbulent flow, can only be used for rough estimation of unsteady friction in laminar flow. A dispersive error appeared during the first pressure peak. The dispersive error occurred in both laminar and turbulent flow cases. The model was not capable of simulating the rounding of the pressure peaks.
- 3) Vardy et al.'s model, originally developed for turbulent flow, can accurately simulate transient friction in turbulent flow cases. However, it gave unsatisfactory results for laminar flows.
- 4) Vardy et al.'s model was modified by introducing a new value for the shear decay coefficient for laminar flows. The modified model proved to be the most accurate model

for simulating transient friction in both laminar and turbulent flows.

Nomenclature

- A is the flow cross sectional area,
- A is the wave speed in a fluid contained within an elastic conduit,
- D is the Pipe diameter,
- E is the Young's Modulus of Elasticity for the pipe material,
- E_j is the modulus of Elasticity of the j th Kelvin-Voigt element,
- e is the pipe wall thickness,
- f is the darcy-Weisbach friction factor,
- g is the gravitational acceleration,
- H is the local flow head ,
- H_b is the barometric pressure head ,
- H_o is the head of the upstream reservoir ,
- $h_f(t)$ is the friction head loss per unit length at time (t),
- N is the number of nodes along the pipe length,
- P is the pressure,
- Q is the volume flow rate,
- R is the pipe radius,
- R_N is the reynolds Number,
- t is the time ,
- V is the flow mean velocity,
- V_o is the steady state flow mean velocity,
- s is the distance along the pipe,
- z is the node elevation from a reference level,
- Δt is the time step in method of characteristics solution,
- λ is the constraint coefficient in the wave speed formula, also used as the multiplier in the solution by the method of characteristics,
- ν is the kinematic viscosity of the fluid,
- ρ is the density of the fluid,
- τ is the dimensionless time in the unsteady friction models ($\tau = \frac{\nu}{R^2} t$).

Subscripts

- L is the condition downstream at time (t- Δt) to be used in the C- characteristic equation,
- P is the node to be calculated at time (t) and
- R is the condition upstream at time (t- Δt) to be used in the C+ characteristic equation.

References

- [1] G. Z., Watters, "Analysis and Control of Unsteady Flow in Pipelines," Second Edition, Butterworths, An Ann Arbor Science Book (1984).
- [2] E. B., Wylie, and V. L., Streeter "Fluid Transients in Systems," Prentice Hall, New Jersey (1993).
- [3] M., Kaplan, V. L., Streeter, and E. B., Wylie, "Computation Of Oil Pipeline Transients," Journal of the Pipeline Division, Proc., ASCE, Vol. 93, (PL3) (1967).
- [4] A., Bergant, and A., Simpson, "Quadratic Equation Inaccuracy For Water Hammer," Journal of Hydraulic Engineering, Vol. 117 (11) (1991).
- [5] P. F., Boulos, D. J. Wood, and J. E., Funk, "A Comparison Of Numerical And Exact Solutions For Pressure Surge Analysis", Proc., 6th International Conference on Pressure Surges, British Hydromechanics Research Association (BHRA), Cranfield, U.K., pp. 149-160 (1990).
- [6] W., Zielke, "Frequency-Dependent Friction In Transient Pipe Flow," Journal of Basic Engineering, Trans. ASME, Vol. 90 (1), pp. 109-115 (1968).
- [7] A. K., Trikha, "An Efficient Method For Simulating Frequency-Dependent Friction In Transient Liquid Flow," Journal of Fluids Engineering, Trans. ASME, Vol. 97 (1), pp. 97-105 (1975).
- [8] K., Suzuki, T., Taketomi, and S., Sato, "Improving Zielke's Method Of Simulating Frequency-Dependent Friction In Laminar Liquid Pipe Flow," Journal of Fluids Engineering, Vol. 113, pp. 569-573 (1991).
- [9] A. E., Vardy, and K. L., Hwang, "A Characteristics Model Of Transient Friction In Pipes," Journal of Hydraulic Research, Vol. 29 (5), pp. 669-684 (1991).
- [10] A. E., Vardy, K. L., Hwang, and J., Brown, "A Weighting Function Model Of Transient Turbulent Pipe Friction," Journal of Hydraulic Research, Vol. 31 (4), pp. 533-548 (1993).
- [11] A. E., Vardy, and J., Brown, "Transient, Turbulent, Smooth Pipe Friction," Journal of Hydraulic Research, Vol. 33 (4), pp. 435-456 (1995).
- [12] B., Brunone, U. M., Golia, and M., Greco, "Some Remarks On The Momentum Equation For Fast Transients," Proc., International Conference On Hydraulic Transients With Water Column Separation, IAHR, Valencia, Spain, pp. 201-209 (1991).
- [13] B., Brunone, U. M., Golia, and M., Greco, "Modeling Of Fast Transients By Numerical Methods," Proc., International Conference On Hydraulic Transients With Water Column Separation, IAHR, Valencia, Spain, pp. 273-280 (1991).
- [14] B., Brunone, U. M., Golia, and M., Greco, "Effects Of Two-Dimensionality On Pipe Transients Modeling," Journal of Hydraulic Engineering, Vol. 121 (12), pp. 906-912 (1995).
- [15] W. F., Silva-Araya, and M. H., Chaudhry, "Computation Of Energy Dissipation In Transient Flow," Journal of Hydraulic Engineering, Vol. 123 (2), pp. 108-115 (1997).
- [16] E. M., Wahba, "The Effect Of Unsteady Friction And Column Separation On Transient Flow In Viscoelastic Pipes," M.Sc. Thesis, Faculty of Engineering, Alexandria University, Egypt (2000).
- [17] E. L., Holmboe, and W. T., Rouleau, "The Effect Of Viscous Shear On Transients In Liquid Lines," Journal of Basic Engineering, Trans. ASME, Vol. 89 (1), pp. 174-180 (1967).

Received July 11, 2001
Accepted October 20, 2001